EARTHQUAKE ENGINEERING AND STRUCTURAL DYNAMICS
Earthquake Engng. Struct. Dyn. **27**, 773–791 (1998)

DYNAMIC ANALYSIS ON STRUCTURES BASE-ISOLATED BY A BALL SYSTEM WITH RESTORING PROPERTY

QIANG ZHOU[1], XILIN LU[1,*], QINGMIN WANG[2], DINGGUO FENG[2] AND QIANFENG YAO[2]
[1]*Research Institute of Engineering Structures, Tongji University, Shanghai 200092, China*
[2]*Department of Civil Engineering, Xi'an University of Architecture & Technology, Xi'an 710055, China*

SUMMARY

A computational model with its analysis method for base-isolated structures by a ball system with restoring property under seismic force is proposed in this paper, and the programs using numerical integration method and incremental harmonic balance method are developed. The analysis method is verified by shaking table test results of a three-storey masonry model. With these programs, the effect of some factors on the aseismic behaviour of base isolation system are analysed, and the comparison of seismic response between structures with and without base isolation is made. Results of both theory and test show that the above-mentioned base isolation system has apparent advantages over the traditional aseismic structures. © 1998 John Wiley & Sons, Ltd.

KEY WORDS: base isolation; ball system with restoring property; numerical integration; incremental harmonic balance method; seismic response

INTRODUCTION

In the traditional aseismic design, it is assumed that every structural member has enough strength to resist seismic force and enough ductility to absorb seismic energy. When this design philosophy is adopted, study shows that the structures absorb plenty of energy and plastic deformation of some structural members is very large. Moreover, it is very difficult to repair and reinforce the structures after an earthquake and it always results in serious damages to indoor devices. Therefore, such kind of structures have become more and more unsatisfactory. Base isolation method as a new aseismic method has been developed since the past few decades. The transmission of ground motion to structures can be effectively controlled and damages to superstructures can be obviously reduced by isolating the structures at their base. In addition, safety of indoor devices is also improved. Theoretical analysis, a model test and on-the-spot measure show that the seismic response can be effectively reduced for the structures with a base isolation system.

Multi-storey brick masonry structure is a major structural form in developing countries. It is very popular in China too. Every seismic attack in the past shows that the seismic performance of brick masonry structures is very bad, and the cost for reinforcing and repairing brick masonry structures is very high. So it is very necessary for brick masonry structures to adopt the base isolation system in high earthquake intensity regions.

* Correspondence to: Xilin Lu, Research Institute of Engineering Structures, Tongji University, 1239 Siping Road, Shanghai 200092, China. E-mail: lxlste@tju.ihep.ac.cn

Contract/grant sponsor: China Southwest Architectural and Research Institute

CCC 0098–8847/98/080773–19$17·50

Received 15 August 1997
Revised 24 November 1997

Now, Pure-Friction (PF) base isolation system and Laminated Rubber Bearing (LRB) base isolation system have been developed widely both in theory and practice.

The PF base isolation system can dissipate the energy of excitation by sliding.[1–6] It is simple and economical and resonance almost does not occur. But the sliding displacement of the superstructure may be large, therefore extra width of the basement is required. Then the price of the basement should be increased. Moreover, various jacks must be used to restore the superstructure after an earthquake.

The LRB base isolation system consists mainly of alternating layers of rubber and steel with the rubber being vulcanized to the steel plates.[6–9] This kind of system is widely adopted practically. Its performance is reliable and easy to control. Moreover, the structures with this kind of system can be restored by itself. But laminated rubber bearings belong to cohesive bearing type which is complex and expensive. So it cannot be accepted by ordinary structures in developing countries. And resonance may occur if LRB base isolation system is designed improperly.

The best technique of isolation is to disconnect the structures from the ground completely when an earthquake occurs. In general, rolling friction is so small that the inertia force of the superstructure is inevitably small. Base isolation by a ball system is proposed on the basis of this idea, as shown in Figure 1.

When the mass of steel balls and sliding friction coefficient are neglected, horizontal force of the mass body is $f = w(\delta' + \delta)/2r$, where w is weight of the mass body, r the radius of the steel ball, δ' and δ the rolling friction coefficients of the upper and lower contact surfaces, respectively. In fact, the rolling friction coefficient is very small. If steel balls are in contact with steel plates, and steel balls and steel plates are well finished and clean, δ' and δ are $0{\cdot}05 \sim 0{\cdot}5$ mm. If r is 100 mm, horizontal force is $f = 0{\cdot}0005 \sim 0{\cdot}005w$, that is, the absolute acceleration of the mass body is only $0{\cdot}005 \sim 0{\cdot}05$ m/s^2. Therefore base isolation by a ball system is very effective. Base isolation by means of free rolling rods under the basement is proposed in paper[10] according to this idea. But there is a obvious defect in this kind of base isolation system, that is, it cannot control the displacement. Various jacks must be used to restore the superstructure after the earthquake. The Friction Pendulum System (FPS), which is developed in the U.S., has gone through extensive analysis and experimental verification since 1986,[11–13] and has led to the implementation, for example, the U.S. Court of Appeals Building in San Francisco.[14] FPS isolators are steel bearings. The internal components consist of a stainless steel concave surface, upon which slides a stainless steel articulated slider surfaced with a high-load capacity, and low friction bearing material composite. Although FPS has a restoring property, it adopts the sliding friction mechanism to reduce seismic force. In general, rolling friction is far less than sliding friction and the former is only about 1/40–1/60 of the later.[15] Combining the advantage of free rolling rod isolators and FPS isolators, the base-isolated by a ball system with restoring property is proposed in paper,[16] as shown in Figure 2.

In order to make a thorough study on this kind of base isolation system, an analysis method for the Multi-Degree-Of-Freedom (MDOF) shear-type structures base-isolated by a ball system with restoring property is proposed based on paper.[17] Shaking table tests on a one-fourth-scale brick masonry structure

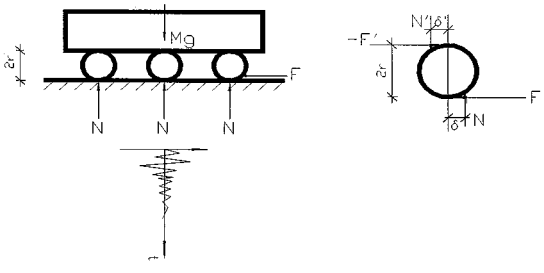

Figure 1. Base-isolated by a ball system without restoring property

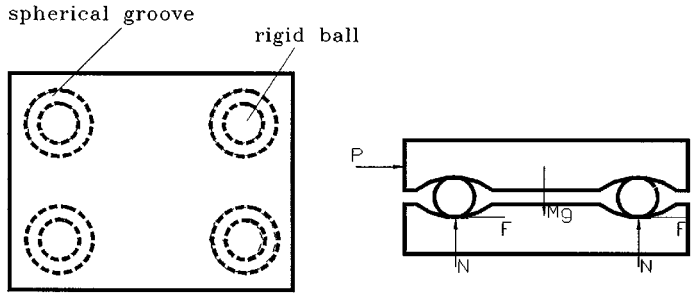

Figure 2. Base-isolated by a ball system with restoring property

with and without the base isolation system are carried out, and the comparison is made between them. To ensure that the comparison is useful, after the tests on the structure with the base isolation system are finished, steel balls are removed, and the model is connected with the shaking table by many bolts. So it is equivalent to the base-fixed structure.

ANALYTICAL FORMULATION

Because the base isolation system is mainly used in brick masonry structures, a superstructure is simplified to a shear-type model with MDOF, as shown in Figure 3.

The following assumptions are adopted in this paper:

(1) Floor slabs and the base plate are rigid bodies, and direction of the floor movement is that of ground motion.
(2) Columns and walls are simplified to weightless elastic straight bar, and axial deformation of the bar is neglected.
(3) The superstructure works in the elastic range under an earthquake.
(4) All spherical grooves and balls have the same type and behaviour.
(5) The balls are regarded as rigid bodies expect when rolling friction coefficient is considered. The balls purely roll along the spherical grooves, and the ball motion is synchronous. So torsion of the superstructure is neglected.
(6) Unidirectional horizontal vibration of the ground is considered, and vertical vibration and torsion of the ground are neglected.

Only one group of basement–ball–superstructure instead of the whole structure is analysed because the balls motion is synchronous.

Weight of the balls is neglected because it is far less than the weight of the superstructure. The governing motion equation of base-isolated N-degree structure subjected to an earthquake acceleration, $\ddot{x}_g$, is given by

$$2(R-r)\left[m_{\mathrm{b}}+\sum_{i=1}^{N} m_i \sin\varphi\left(\frac{\delta}{r}\cos\varphi\,\mathrm{sgn}(\dot{\varphi})+\sin\varphi\right)\right]\ddot{\varphi}+2(R-r)\dot{\varphi}^2$$

$$\times\left[m_{\mathrm{b}}\frac{\delta}{r}\mathrm{sgn}(\dot{\varphi})+\sum_{i=1}^{N} m_i \cos\varphi\left(\frac{\delta}{r}\cos\varphi\,\mathrm{sgn}(\dot{\varphi})+\sin\varphi\right)\right]+\left(m_{\mathrm{b}}+\sum_{i=1}^{N} m_i\right)g$$

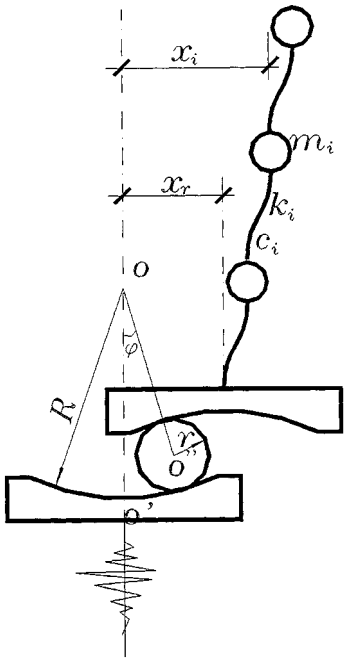

Figure 3. Computational model of the base-isolated structure

$$\times\left(\frac{\delta}{r}\cos\varphi\,\mathrm{sgn}(\dot{\varphi})+\sin\varphi\right)+[k_1(x_1-x_r)+c_1(\dot{x}_1-\dot{x}_r)-m_b\ddot{x}_g]$$

$$\times\left(\frac{\delta}{r}\sin\varphi\,\mathrm{sgn}(\dot{\varphi})-\cos\varphi\right)=0 \tag{1}$$

$$m_1\ddot{x}_1+(c_1+c_2)\dot{x}_1-c_2\dot{x}_2-c_1\dot{x}_r+(k_1+k_2)x_1-k_2x_2-k_1x_r=-m_1\ddot{x}_g \tag{2}$$

$$m_i\ddot{x}_i-c_i\dot{x}_{i-1}+(c_i+c_{i+1})\dot{x}_i-c_{i+1}\dot{x}_{i+1}-k_ix_{i-1}+(k_i+k_{i+1})x_i-k_{i+1}x_{i+1}=-m_i\ddot{x}_g$$

$$(i=2,3,\ldots,N-1) \tag{3}$$

$$m_N\ddot{x}_N-c_N\dot{x}_{N-1}+c_N\dot{x}_N-k_Nx_{N-1}+k_Nx_N=-m_N\ddot{x}_g \tag{4}$$

where

$$x_r=2(R-r)\sin\varphi,\qquad \dot{x}_r=2(R-r)\cos\dot{\varphi}\cdot\dot{\varphi} \tag{5}$$

By solving equations (1)–(4), the displacement, acceleration and internal force of every element of the structure base-isolated by a ball system with restoring property can be obtained at any time under an earthquake. The equations of motion are mutual coupling and strong non-linear equations, therefore, Numerical Integration (NI) method and Incremental Harmonic Balance (IHB) method are used to solve them.

DYNAMIC ANALYSIS USING NI METHOD

Because the term of $\dot{\varphi}^2$ and $\mathrm{sgn}(\dot{\varphi})$ are included in the equations of motion, proper modification is necessary.

The state vector is introduced as follows:

$$\begin{aligned} y_1 &= \varphi \\ y_2 &= \dot{\varphi} \\ y_3 &= x_1 \\ y_4 &= \dot{x}_1 \\ &\vdots \\ y_{2i+1} &= x_i \\ y_{2i+2} &= \dot{x}_i \\ &\vdots \\ y_{2N+1} &= x_N \\ y_{2N+2} &= \dot{x}_N \end{aligned} \tag{6}$$

By substituting equation (6) into the equations of motion (1)–(4), the equation of state can be obtained. It is completely expressed as follows:

$$\begin{aligned} \dot{y}_1 &= y_2 \\ \dot{y}_2 &= -\left\{2(R-r)y_2^2\left[m_\mathrm{b}\frac{\delta}{r}\mathrm{sgn}(y_2) + \sum_{i=1}^{N} m_i \cos y_1\left(\frac{\delta}{r}\cos y_1\,\mathrm{sgn}(y_2) + \sin y_1\right)\right]\right. \\ &\quad + \left(m_\mathrm{b} + \sum_{i=1}^{N} m_i\right) g\left(\frac{\delta}{r}\cos y_1\,\mathrm{sgn}(y_2) + \sin y_1\right) + [k_1(y_3 - 2(R-r)\sin y_1) \\ &\quad \left. + c_1(y_4 - 2(R-r)\cos y_1 y_2) - m_\mathrm{b}\ddot{x}_g]\left(\frac{\delta}{r}\sin y_1\,\mathrm{sgn}(y_2) - \cos y_1\right)\right\} \Big/ \left\{2(R-r)\right. \\ &\quad \left. \times\left[m_\mathrm{b} + \sum_{i=1}^{N} m_i \sin y_1\left(\frac{\delta}{r}\cos y_1\,\mathrm{sgn}(y_2) + \sin y_1\right)\right]\right\} \\ \dot{y}_3 &= y_4 \\ \dot{y}_4 &= -[c_1(y_4 - 2(R-r)\cos y_1 y_2) + k_1(y_3 - 2(R-r)\sin y_1) - c_2(y_6 - y_4) \\ &\quad - k_2(y_5 - y_3)]/m_1 - \ddot{x}_g \\ &\vdots \\ \dot{y}_{2i+1} &= \dot{y}_{2i+2} \\ \dot{y}_{2i+2} &= [c_i y_{2i} - (c_i + c_{i+1})y_{2i+2} + c_{i+1}y_{2i+4} + k_i y_{2i-1} - (k_i + k_{i+1})y_{2i+1} \\ &\quad + k_{i+1}y_{2i+3}]/m_i - \ddot{x}_g \\ &\vdots \\ \dot{y}_{2N+1} &= y_{2N+2} \\ \dot{y}_{2N+2} &= (c_N y_{2N} - c_N y_{2N+2} + k_N y_{2N-1} - k_N y_{2N+1})/m_N - \ddot{x}_g \end{aligned} \tag{7}$$

Now, the equations of motion (1)–(4) are changed into $\dot{\tilde{Y}} = \tilde{f}(\tilde{Y})$, therefore, the fourth-order Runge–Kutta method can be used to solve equation (7).

DYNAMIC ANALYSIS USING IHB METHOD

In order to study the effects induced by changing some parameters and to carry on frequency-response analysis for the structures, IHB method is used. The IHB method was presented in 1981,[18] and it has been developed further and was successfully applied to the analysis of periodic and almost periodic non-linear structural vibrations and related problems.[19–22] The most important advantages of the IHB method is that it is capable of dealing with a strongly non-linear system to any desired accuracy. Furthermore, the IHB method is a general computer method for finding the periodic solution of a non-linear differential equation. According to paper,[19–22] a multi-harmonic solution of the structures base-isolated by a ball system with restoring property is obtained with the IHB method.

At first, the equations of motion (1)–(4) should be changed into a dimensionless form.

The seismic wave is assumed as a cosine wave, that is $\omega_0^2 Dp \cos \omega t$, where p is dimensionless, D is the characteristic length, $\omega_0^2 = g/2(R - r)$.

Let

$$x_i = Du_i \ (i = 1, 2, 3, \ldots, N) \tag{8}$$

A dimensionless time, τ, is adopted as the new independent variable to determine the subharmonic vibration of order $1/\lambda$, λ being a positive integer. Let

$$\lambda\tau = \omega t \tag{9}$$

λ is taken as unity when the harmonic and superharmonic vibration are sought. While λ is greater than unity when the subharmonic vibration is required:

Let

$$\frac{k_1}{m_b} = \beta_0\omega_0^2, \quad \frac{c_1}{m_b} = \alpha_0\omega_0$$

$$\frac{k_1}{m_1} = \beta_{11}\omega_1^2, \quad \frac{k_2}{m_1} = \beta_{12}\omega_1^2, \quad \frac{c_1}{m_1} = \alpha_{11}\omega_1, \quad \frac{c_2}{m_1} = \alpha_{12}\omega_1$$

$$\frac{k_i}{m_i} = \beta_{ii}\omega_i^2, \quad \frac{k_{i+1}}{m_i} = \beta_{i,i+1}\omega_i^2, \quad \frac{c_i}{m_i} = \alpha_{ii}\omega_i, \quad \frac{c_{i+1}}{m_i} = \alpha_{i,i+1}\omega_i$$

$$\frac{k_N}{m_N} = \beta_N\omega_N^2, \quad \frac{c_N}{m_N} = \alpha_N\omega_N$$

$$\Omega_j = \frac{\omega}{\omega_j}, \tag{10}$$

$(i = 2, 3, \ldots, N-1, j = 0, 1, 2, \ldots, N)$

where $\omega_j (j = 1, 2, \ldots, N)$ is the jth natural frequency of the base-fixed structure.

Substituting equations (8)–(10) into equations (1)–(4), the following equations are obtained:

$$q_0 = \left[1 + \frac{\sum_{i=1}^{N} m_i}{m_b} \sin\varphi \left(\frac{\delta}{r}\cos\varphi\,\mathrm{sgn}(\dot{\varphi}) + \sin\varphi\right)\right]\frac{\Omega_0^2}{\lambda^2}\ddot{\varphi} + \frac{\Omega_0^2}{\lambda^2}\dot{\varphi}^2$$
$$\times\left[\frac{\delta}{r}\mathrm{sgn}(\dot{\varphi}) + \frac{\sum_{i=1}^{N} m_i}{m_b}\cos\varphi\left(\frac{\delta}{r}\cos\varphi\,\mathrm{sgn}(\dot{\varphi}) + \sin\varphi\right)\right] + \frac{(\sum_{i=1}^{N} m_i + m_b)}{m_b}$$
$$\times\left(\sin\varphi + \frac{\delta}{r}\cos\varphi\,\mathrm{sgn}(\dot{\varphi})\right) + \frac{1}{2(R-r)}\left[\beta_0(Du_1 - 2(R-r)\sin\varphi) + \alpha_0\frac{\Omega_0}{\lambda}(D\dot{u}_1\right.$$
$$\left. - 2(R-r)\cos\varphi\dot{\varphi}\right) - Dp\cos\lambda\tau\left]\left(\frac{\delta}{r}\sin\varphi\,\mathrm{sgn}(\dot{\varphi}) - \cos\varphi\right) = 0 \right. \tag{11}$$

$$q_1 = \frac{\Omega_1^2}{\lambda^2}\ddot{u}_1 + \alpha_{11}\frac{\Omega_1}{\lambda}\left(\dot{u}_1 - \frac{2(R-r)}{D}\cos\varphi\dot{\varphi}\right) + \beta_{11}\left(u_1 - \frac{2(R-r)}{D}\sin\varphi\right)$$
$$- \alpha_{12}\frac{\Omega_1}{\lambda}(\dot{u}_2 - \dot{u}_1) - \beta_{12}(u_2 - u_1) + p\frac{\omega_0^2}{\omega_1^2}\cos\lambda\tau = 0 \tag{12}$$

$$q_i = \frac{\Omega_i^2}{\lambda^2}\ddot{u}_i - \alpha_{ii}\frac{\Omega_i}{\lambda}\dot{u}_{i-1} + (\alpha_{ii} + \alpha_{i,i+1})\frac{\Omega_i}{\lambda}\dot{u}_i - \alpha_{i,i+1}\frac{\Omega_i}{\lambda}\dot{u}_{i+1} - \beta_{ii}u_{i-1}$$
$$+ (\beta_{ii} + \beta_{i,i+1})u_i - \beta_{i,i+1}u_{i+1} + p\frac{\omega_0^2}{\omega_i^2}\cos\lambda\tau = 0 \quad (i = 2,3,4,\ldots,N-1) \tag{13}$$

$$q_N = \frac{\Omega_N^2}{\lambda^2}\ddot{u}_N - \alpha_N\frac{\Omega_N}{\lambda}\dot{u}_{N-1} + \alpha_N\frac{\Omega_N}{\lambda}\dot{u}_N - \beta_N u_{N-1} + \beta_N u_N + p\frac{\omega_0^2}{\omega_N^2}\cos\lambda\tau = 0 \tag{14}$$

where the dot denotes differentiation with respect to the dimensionless time τ.

Let

$$\begin{cases}\{X\} = [\varphi \quad u_1 \quad u_2 \quad \cdots \quad u_N]^{\mathrm{T}} \\ \{Q\} = [q_0 \quad q_1 \quad q_2 \quad \cdots \quad q_N]^{\mathrm{T}}\end{cases} \tag{15}$$

After expanding equations (11)–(14) in a Taylor's series around the initial state, the linearized incremental equation produced by ignoring all the non-linear terms in small increments are found to be

$$\frac{\partial\tilde{Q}}{\partial\ddot{\tilde{X}}}\Delta\ddot{\tilde{X}} + \frac{\partial\tilde{Q}}{\partial\dot{\tilde{X}}}\Delta\dot{\tilde{X}} + \frac{\partial\tilde{Q}}{\partial\tilde{X}}\Delta\tilde{X} = -\tilde{Q}_0 - \frac{\partial\tilde{Q}}{\partial p}\Delta p - \frac{\partial\tilde{Q}}{\partial\Omega_0}\Delta\Omega_0 \tag{16}$$

Where $\tilde{Q}_0$ is the modified term, if the real solution of equation (16) can be obtained, $\tilde{Q}_0 \equiv \tilde{0}$.

The steady periodic solution of equation (16) including subharmonic, superharmonic and harmonic vibrations, can be written as the Fourier series:

$$X_i = a_{i0} + \sum_{k=1}^{M}(a_{ik}\cos k\tau + b_{ik}\sin k\tau)$$
$$(i = 1,2,\ldots,N+1) \tag{17}$$
$$\Delta X_i = \Delta a_{i0} + \sum_{k=1}^{M}(\Delta a_{ik}\cos k\tau + \Delta b_{ik}\sin k\tau)$$

Substituting equation (17) into equation (16), and applying the Galerkin procedure for one period, one obtains

$$\int_0^{2\pi}\left[\frac{\partial\tilde{Q}}{\partial\tilde{\ddot{X}}}\Delta\tilde{\ddot{X}}+\frac{\partial\tilde{Q}}{\partial\tilde{\dot{X}}}\Delta\tilde{\dot{X}}+\frac{\partial\tilde{Q}}{\partial\tilde{X}}\Delta\tilde{X}\right]\begin{Bmatrix}1\\ \cos k\tau\\ \sin k\tau\\ 1\\ \cos k\tau\\ \vdots\\ \sin k\tau\end{Bmatrix}\mathrm{d}\tau=\int_0^{2\pi}\left[-\tilde{Q}_0-\frac{\partial\tilde{Q}}{\partial p}\Delta p-\frac{\partial\tilde{Q}}{\partial\Omega_0}\Delta\Omega_0\right]\begin{Bmatrix}1\\ \cos k\tau\\ \sin k\tau\\ 1\\ \cos k\tau\\ \vdots\\ \sin k\tau\end{Bmatrix}\mathrm{d}\tau$$

$$(k=1,2,\ldots,M) \tag{18}$$

Amplitude vector is defined as

$$\begin{cases}\tilde{a}=[a_{10}\ \ a_{11}\ \cdots\ a_{1M}\ \ b_{11}\ \cdots\ b_{1M}\ \ a_{20}\ \cdots\ b_{N+1,M}]^{\mathrm{T}}\\ \Delta\tilde{a}=[\Delta a_{10}\ \ \Delta a_{11}\ \cdots\ \Delta a_{1M}\ \ \Delta b_{11}\ \cdots\ \Delta b_{1M}\ \ \Delta a_{20}\ \cdots\ \Delta b_{N+1,M}]^{\mathrm{T}}\end{cases} \tag{19}$$

Substituting equation (19) into equation (18), a set of linear equation in terms of $\Delta\tilde{a}$, $\Delta\omega$ and Δp can be easily obtained

$$[D]\,\Delta\tilde{a}=-\tilde{R}-\Delta\Omega_0\,\tilde{\Omega}-\Delta p\tilde{p} \tag{20}$$

where $[D], \tilde{R}, \Omega, \tilde{p}$ are given in detail in the appendix.

It is worth mentioning that in equation (20) the number of incremental unknown is greater than the number of equations available due to the existence of Δp and $\Delta\Omega_0$. However, since one is primarily interested in the frequency-response curve of the system for a constant force level, p is fixed as a parameter, which implies $\Delta p = 0$. Hence, equation (20) is reduced to

$$[D]\Delta\tilde{a}=-\tilde{R}-\Delta\Omega_0\tilde{\Omega}. \tag{21}$$

If $\Delta\Omega_0$ is specified as a control increment, then Ω_0 remains constant through the iteration process, i.e. $\Delta\Omega_0 = 0$, while other increments are solved from the equation

$$[D]\Delta\tilde{a}=-\tilde{R}. \tag{22}$$

After $\Delta\tilde{a}$ is obtained, let $\tilde{a}^{(i)}=\tilde{a}^{(i-1)}+\Delta\tilde{a}$, then substitute $\tilde{a}^{(i)}$ into equation (22) and get another $\Delta\tilde{a}$. This iteration process is repeated until the magnitude of the corrected vector $\tilde{R}$ is acceptably small, in which case a solution is obtained. The value of Ω_0 is then added by an increment $\Delta\Omega_0$ artificially, and a new iteration is repeated with the new value of Ω_0 until a new solution is obtained. Then one can obtain the frequency-response curve.

If one is interested in the forcing amplitude response curve of the system for a constant frequency level, frequency is fixed, then $\Delta\Omega_0 = 0$. Hence, equation (20) is reduced to

$$[D]\Delta\tilde{a}=-\tilde{R}-\Delta p\tilde{p} \tag{23}$$

Similarly, one can obtain the forcing amplitude response curve.

THE BRICK MASONRY MODEL TEST

To study the aseismic behaviour of the structures base-isolated by a ball system with restoring property and to verify the correctness of the equation of motion and the analysis method, a shaking table test on a one-fourth scale brick masonry model with and without the base isolation system was carried out on the basis of paper [17].

The brick masonry model was three storeys and one bay. Each storey height was 750 mm, and total height was 2250 mm. The plan size of the model was 1200×900 mm. Depth-width ratio was 1·875. Details of the model are shown in Figure 4.

The model was made of model brick and mixed mortar. Model brick was obtained by cutting the machine-made brick, and its size was $115 \times 50 \times 30$ mm. The cube strength of mixed mortar was 10 MPa, and its mixture proportion was cement : lime : sand = 195 : 117 : 1450 (weight ratio/m^3). The model was built with conventional methods, and the cube strength of concrete was 20 Mpa.

The floor slabs and base plate of the model were precast reinforced concrete slabs, which were 40 mm and 150 mm thick respectively. Cast-in-place concrete ring beam, whose section size was 50×45 mm, was set under every floor level. The plan size of the base plate is 1800×1500 mm. Curvature radius and arc-length of the steel spherical grooves which were inlaid into the base plate were $R = 700$ mm and $a = 400$ mm, respectively. Radius of the steel ball was $r = 100$ mm. Four square piers with a dimension of 600×600 mm were fixed to the shaking table with bolts. Size, material and position of the spherical grooves which were inlaid into the piers were the same as those of the base plate.

Simplified profile of the shaking table experiment of the model with the base isolation is shown in Figure 5.

Acceleration meters, which record absolute acceleration time history, were put on the shaking table, top-floor and mid-floor of the model.

First, the base-isolated model test was done and then the base-fixed model test. The exciting seismic wave of the test was EL-centro earthquake record (1940 N-S). The comparisons of the model with and without the base isolation system are shown in Table I.

Where

$$\mathrm{TR} = \frac{\text{absolute acceleration of 3rd floor}}{\text{shaking table acceleration}}$$

It is seen that the base isolation system can obviously reduce structural response. It was also observed that when shaking table acceleration was 359·8 gal, there was no crack in the base-isolated model; But when shaking table acceleration was 100·0 gal, there was some crack in the base-fixed model, and when shaking table acceleration was 533·3 gal, serious diagonal cracks occurred in the transverse walls of the first storey of the model and the model was seriously damaged. It proved that the above mentioned base isolation system is effective.

NUMERICAL ANALYSIS OF BASE-ISOLATED STRUCTURES

1. Verification of the equation of motion

A program using the NI method and the IHB method are made based on the obtained equation of motion.

Some important parameters of the brick masonry model are input to the program using the NI method, so one can observe whether the computation results are approximately equal to the test results. Then one can determine whether the equation of motion is reasonable.

Using the extended Kalman filter method,[23] stiffness and damping of the brick masonry model are identified, as shown in Table II.

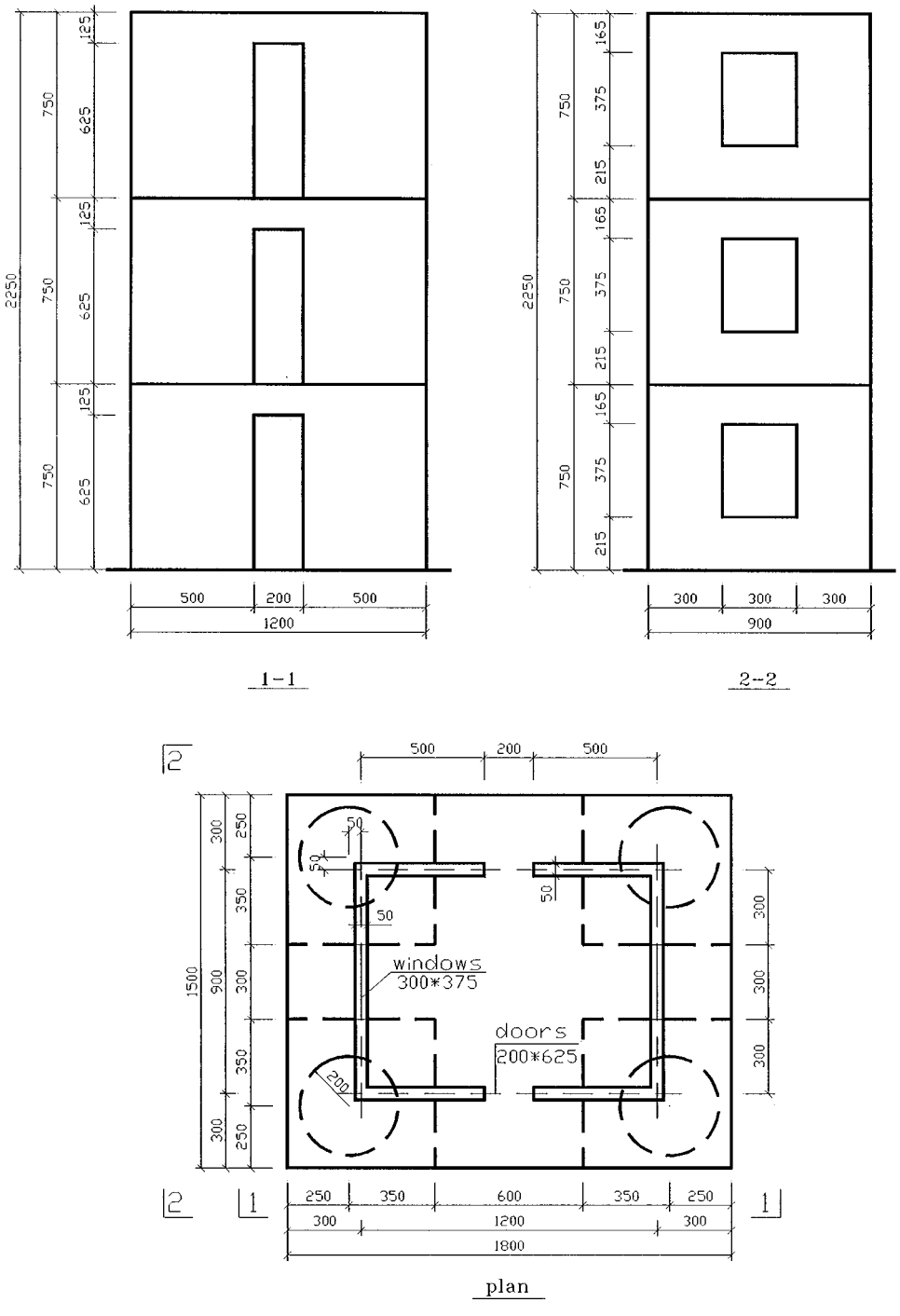

Figure 4. Details of the brick masonry model (Note: all dimensions in mm)

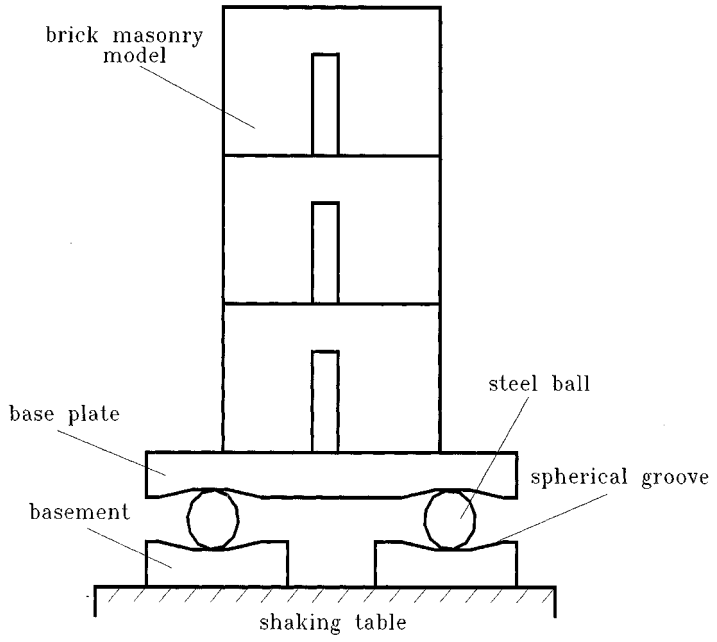

Figure 5. Simplified profile of the base-isolated model

Table I. Absolute acceleration of the model

Working state	Shaking table (gal)	2nd floor (gal)	3rd floor (gal)	Transmitted ratio (TR)
Base-fixed	339·2	403·0	523·0	1·542
Base-isolated	359·8	108·0	177·7	0·494

Table II. Structural parameters of the model

	Mass (kg)	Stiffness (N/mm)	Damping (N s/mm)
1st floor	678·6	11839·2	96·4
2nd floor	678·6	3591·9	5·6
3rd floor	559·3	6393·6	44·0
Base plate	1352·3		

Let $\delta = 0{\cdot}4$ mm, top-floor relative acceleration time history of the base-isolated model under EL-centro earthquake record (1940 N-S), whose maximum acceleration is 359·8 gal, are obtained as shown in Figure 6(a), in which the solid line represents the theoretical results and the dashed line the test results. Theoretical response curves coincides well with test curves. It shows that the program and motion equation are correct.

In order to verify the program using the IHB method, one should make a comparison between the two groups of computational results which are obtained from the program using the NI method and the program using the IHB method respectively under the same condition, that is, the same structure is excited by the same seismic wave. When the structure is excited by a cosine wave, whose frequency is 18·84 Hz and amplitude is 98·0 gal, two groups of results are obtained and compared, as shown Figure 6(b), in which the

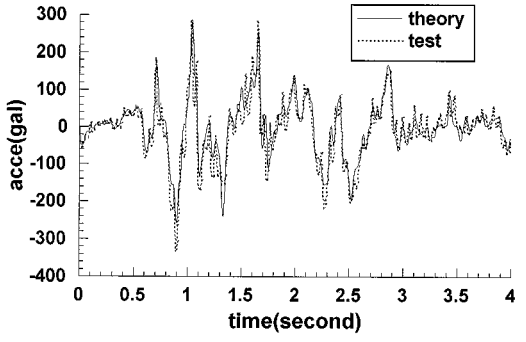

(a) Comparison between theory and test

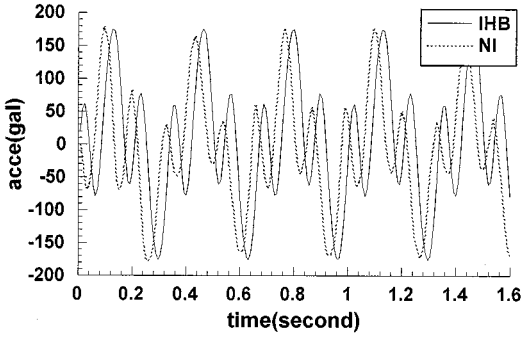

(b) Comparison between IHB method and NI method

Figure 6. Verification of the motion equation and analysis method

solid line represents results with the IHB method and the dashed line results with the NI method. From this figure, validity of the program using the IHB method is verified.

2. Effects of some parameters

With the program using the IHB method, the effects of some parameters on the acceleration and displacement response of the base isolation system are analysed.

Take a three-degree model for example. Parameters of the model and base isolation device are listed as follows:

Radius of the spherical groove $R = 0{\cdot}7$ m; radius of the rigid ball $r = 0{\cdot}21$ m; rolling friction coefficient $\delta = 2{\cdot}5 \times 10^{-3}$ m; mass of the base plate $m_b = 1500$ kg; mass, stiffness and damping of the superstructure are 650 kg, $1{\cdot}0 \times 10^6$ N/m and 4583·0 N s/m, respectively; the excited wave is a cosine wave with 49·0 gal.

The fundamental frequency of the base-fixed model is 17·456 rad/s, and generalized damping ratio of the first mode $\xi = 0{\cdot}04$, and the natural frequency of the base isolation device $\omega_0 = \sqrt{g/2(R-r)} = 3{\cdot}16$ rad/s.

The effects of five kind of parameters, which are the rolling friction coefficient δ, radius of the spherical groove R, radius of the rigid ball r, mass of the base plate m_b and stiffness of the superstructure K, on the acceleration and displacement responses of the base-isolated structure are obtained, as shown from Figures 7 to 11.

From these figures, one can observe that when the excited frequency is around the natural frequency of the base isolation device, which is 3·16 rad/s in Figure 7 and are 3·94, 3·54 and 3·16 rad/s, respectively, in Figure 8 and so on, the responses of the base isolation system sharply increase, that is, there exists resonance. In

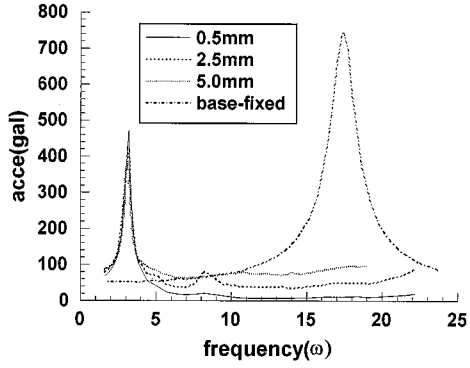

(a) 3rd floor absolution acceleration

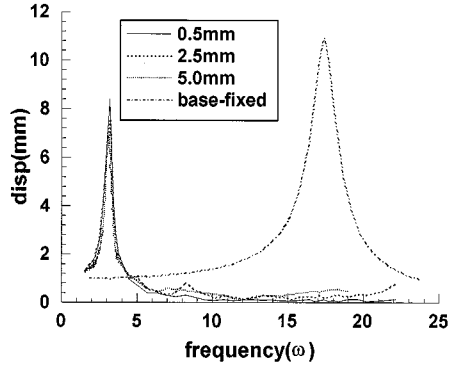

(b) 1st floor interstory drift

Figure 7. Comparison between different friction coefficients δ

general, predominant frequency of the seismic wave is more than 1·0 Hz, i.e. 6.28 rad/s, so if the parameters of the base isolation device are properly selected, resonance can be avoided. One can also discover that the responses of the base isolation system are far less than those of the base-fixed structure if the excited frequency is more than 5·0 rad/s.

So two conclusions can be obtained:

(a) Resonance may occur when the structure base-isolated by a ball system with restoring property is excited by some seismic wave. But the resonant frequency is only related to the vibration frequency of the base isolation device, and is almost irrelevant to the dynamic character of the superstructure. Because the predominant frequency of the seismic wave is often no less than 1.0 Hz, the parameters of the base isolation device should be properly selected, so as to make its natural frequency far from the predominant frequency of the seismic wave, thus the aseismic capacity of the base isolation system can be highly improved.

(b) If resonance is not considered, the rolling friction coefficient, radius of the rigid ball, and mass of the base plate have a great effect on the response of the base-isolated structure, while radius of the spherical groove has little effect on it.

3. Aseismic behaviour comparison

Take a six-degree model for example. Mass, stiffness and damping of the model are 650 kg, 2000 N/mm and 12·0 N s/mm, respectively.

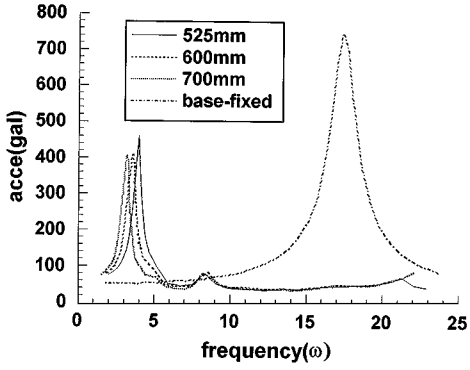

(a) 3rd floor absolution acceleration

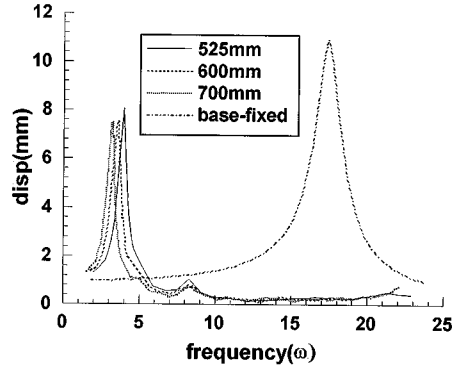

(b) 1st floor interstory drift

Figure 8. Comparison between different radii of the spherical groove R

The parameters of the base isolation device are same as the above-mentioned device.

The fundamental frequency of the base-fixed structure is 2·182 Hz, and generalized damping ratio of the first mode $\xi = 0{\cdot}04$.

With the program using the NI method, response curves of a six-degree model with and without the base-isolation system under EL-centro earthquake record (1940 N-S), whose amplitude is 125·0, 250·0 and 500·0 gal, respectively, are calculated, and the comparison is made between them as shown in Figure 12. It shows that the base isolation system has apparent advantages over the traditional aseismic structure.

CONCLUSIONS

The conclusions emerging from this work are the following:

1. The motion equation for base-isolated structures by a ball system with restoring property is proposed.
2. Because the equations of motion are mutually coupling and strong non-linear equations, the Numerical Integration (NI) method and the Incremental Harmonic Balance (IHB) method are used to solve them. Using the NI method, the displacement, acceleration and internal force of every element of the base-isolated structure can be obtained at any time under the seismic wave. And with a program using the IHB method, the effects of some parameters on the aseismic behaviour of the base isolation system can be analysed.

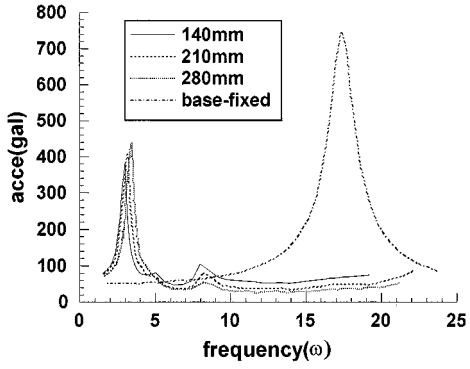

(a) 3rd floor absolution acceleration

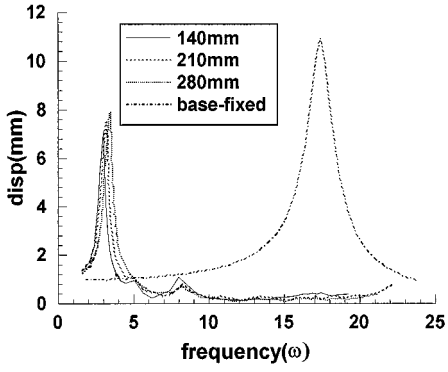

(b) 1st floor interstory drift

Figure 9. Comparison between different radii of the ball r

3. The equations of motion and the analysis method for the base-isolated structure are verified by the shaking table test results of a three-storey masonry model.
4. By comparison with seismic response of traditional base-fixed structures, results of both theory and tests show that the responses of structures base-isolated by a ball system with restoring property can be reduced significantly. At the same time, numerical analysis shows that resonance may occur when the structure is excited by some seismic wave. But the resonant frequency is only related to the vibration frequency of the base isolation device, and is almost irrelevant to the dynamic character of the structure. By properly adjusting some parameters of the base isolation device, so as to make its natural frequency far from the predominant frequency of the seismic wave, then the aseismic capacity of the base-isolated structure can be highly improved. Moreover, the rolling friction coefficient, radius of the rigid ball and mass of the base plate have a great effect on the response of base-isolated structures, while the radius of the spherical groove has little effect on it.

APPENDIX

$$\tilde{R} = \left[\int_0^{2\pi} Q_{10}\,\mathrm{d}\tau, \quad \int_0^{2\pi} Q_{10}\cos k\tau\,\mathrm{d}\tau, \quad \int_0^{2\pi} Q_{10}\sin k\tau\,\mathrm{d}\tau, \quad \int_0^{2\pi} Q_{20}\,\mathrm{d}\tau, \quad \int_0^{2\pi} Q_{20}\cos k\tau\,\mathrm{d}\tau, \right.$$
$$\left. \int_0^{2\pi} Q_{20}\sin k\tau\,\mathrm{d}\tau \quad \cdots \quad \int_0^{2\pi} Q_{N+1,0}\sin k\tau\,\mathrm{d}\tau \right]^{\mathrm{T}}$$

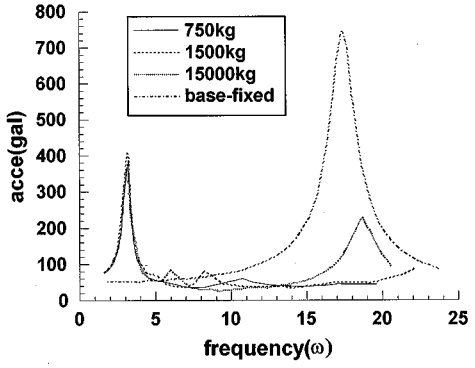

(a) 3rd floor absolution acceleration

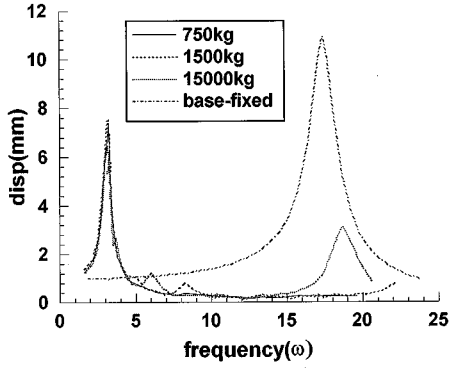

(b) 1st floor interstory drift

Figure 10. Comparison between different masses of the base plate m_b

$$\tilde{Q} = \left[\int_0^{2\pi} \frac{\partial Q_1}{\partial \Omega_0} \mathrm{d}\tau, \quad \int_0^{2\pi} \frac{\partial Q_1}{\partial \Omega_0} \cos k\tau \, \mathrm{d}\tau, \quad \int_0^{2\pi} \frac{\partial Q_1}{\partial \Omega_0} \sin k\tau \, \mathrm{d}\tau, \quad \int_0^{2\pi} \frac{\partial Q_2}{\partial \Omega_0} \mathrm{d}\tau, \right.$$

$$\left. \int_0^{2\pi} \frac{\partial Q_2}{\partial \Omega_0} \cos k\tau \, \mathrm{d}\tau, \quad \int_0^{2\pi} \frac{\partial Q_2}{\partial \Omega_0} \sin k\tau \, \mathrm{d}\tau \quad \cdots \quad \int_0^{2\pi} \frac{\partial Q_{N+1}}{\partial \Omega_0} \sin k\tau \, \mathrm{d}\tau \right]^{\mathrm{T}}$$

$$\tilde{P} = \left[\int_0^{2\pi} \frac{\partial Q_1}{\partial p} \mathrm{d}\tau, \quad \int_0^{2\pi} \frac{\partial Q_1}{\partial p} \cos k\tau \, \mathrm{d}\tau, \quad \int_0^{2\pi} \frac{\partial Q_1}{\partial p} \sin k\tau \, \mathrm{d}\tau, \quad \int_0^{2\pi} \frac{\partial Q_1}{\partial p} \mathrm{d}\tau, \right.$$

$$\left. \int_0^{2\pi} \frac{\partial Q_1}{\partial p} \cos k\tau \, \mathrm{d}\tau, \quad \int_0^{2\pi} \frac{\partial Q_1}{\partial p} \sin k\tau \, \mathrm{d}\tau \quad \cdots \quad \int_0^{2\pi} \frac{\partial Q_{N+1}}{\partial p} \sin k\tau \, \mathrm{d}\tau \right]^{\mathrm{T}}$$

$$[D] = \begin{bmatrix} [D_{11}] & [D_{12}] & \cdots & [D_{1,N+1}] \\ [D_{21}] & [D_{22}] & \cdots & [D_{2,N+1}] \\ \vdots & \vdots & & \vdots \\ [D_{N+1,1}] & [D_{N+1,2}] & \cdots & [D_{N+1,N+1}] \end{bmatrix}, \quad [D_{ij}] = [A_{ij}] + [B_{ij}] + [C_{ij}]$$

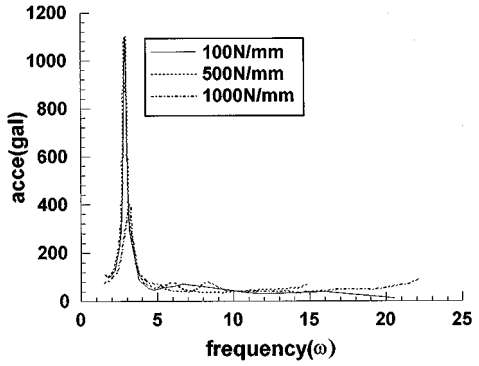

(a) 3rd floor absolution acceleration

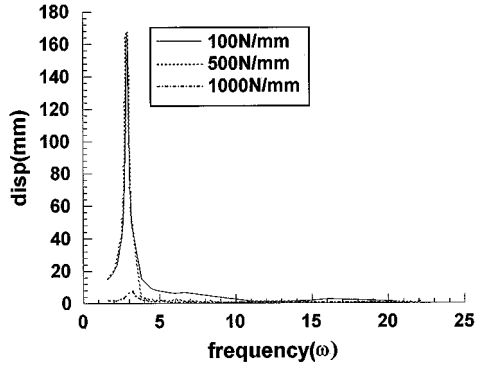

(b) 1st floor interstory drift

Figure 11. Comparison between different structural stiffnesses K

$$[A_{ij}] = \begin{bmatrix} 0 & \int_0^{2\pi} \frac{\partial Q_i}{\partial X_j}(-m^2\cos m\tau)\,\mathrm{d}\tau & \int_0^{2\pi} \frac{\partial Q_i}{\partial X_j}(-m^2\sin m\tau)\,\mathrm{d}\tau \\ \tilde{0} & \int_0^{2\pi} \frac{\partial Q_i}{\partial \ddot{X}_j}\cos k\tau(-m^2\cos m\tau)\,\mathrm{d}\tau & \int_0^{2\pi} \frac{\partial Q_i}{\partial \ddot{X}_j}\cos k\tau(-m^2\sin m\tau)\,\mathrm{d}\tau \\ \tilde{0} & \int_0^{2\pi} \frac{\partial Q_i}{\partial \ddot{X}_j}\sin k\tau(-m^2\cos m\tau)\,\mathrm{d}\tau & \int_0^{2\pi} \frac{\partial Q_i}{\partial \ddot{X}_j}\sin k\tau(-m^2\sin m\tau)\,\mathrm{d}\tau \end{bmatrix}$$

$$[B_{ij}] = \begin{bmatrix} 0 & \int_0^{2\pi} \frac{\partial Q_i}{\partial \dot{X}_j}(-m\sin m\tau)\,\mathrm{d}\tau & \int_0^{2\pi} \frac{\partial Q_i}{\partial \dot{X}_j}(m\cos m\tau)\,\mathrm{d}\tau \\ \tilde{0} & \int_0^{2\pi} \frac{\partial Q_i}{\partial \dot{X}_j}\cos k\tau(-m\sin m\tau)\,\mathrm{d}\tau & \int_0^{2\pi} \frac{\partial Q_i}{\partial \dot{X}_j}\cos k\tau(m\cos m\tau)\,\mathrm{d}\tau \\ \tilde{0} & \int_0^{2\pi} \frac{\partial Q_i}{\partial \dot{X}_j}\sin k\tau(-m\sin m\tau)\,\mathrm{d}\tau & \int_0^{2\pi} \frac{\partial Q_i}{\partial \dot{X}_j}\sin k\tau(m\cos m\tau)\,\mathrm{d}\tau \end{bmatrix}$$

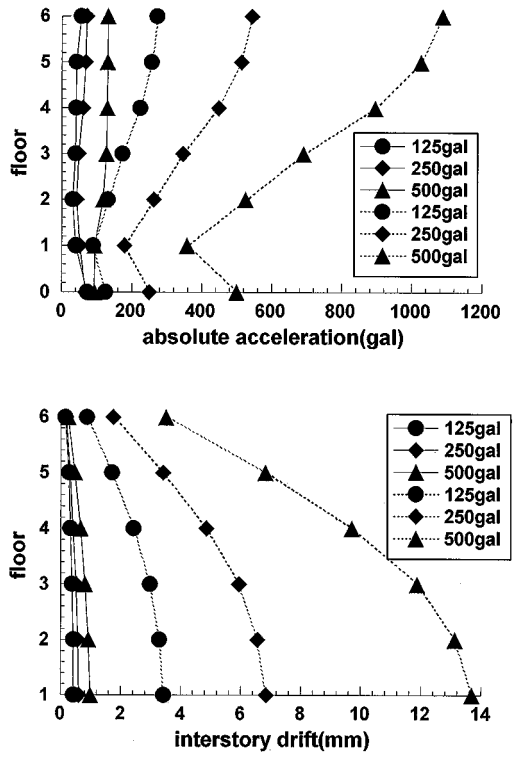

Figure 12. Comparison between with and without base isolation system (—— base-isolated, – – – – base-fixed)

$$[C_{ij}] = \begin{bmatrix} \int_0^{2\pi} \frac{\partial Q_i}{\partial X_j} \mathrm{d}\tau & \int_0^{2\pi} \frac{\partial Q_i}{\partial X_j} \cos m\tau \, \mathrm{d}\tau & \int_0^{2\pi} \frac{\partial Q_i}{\partial X_j} \sin m\tau \, \mathrm{d}\tau \\ \int_0^{2\pi} \frac{\partial Q_i}{\partial X_j} \cos k\tau \, \mathrm{d}\tau & \int_0^{2\pi} \frac{\partial Q_i}{\partial X_j} \cos k\tau \cos m\tau \, \mathrm{d}\tau & \int_0^{2\pi} \frac{\partial Q_i}{\partial X_j} \cos k\tau \sin m\tau \, \mathrm{d}\tau \\ \int_0^{2\pi} \frac{\partial Q_i}{\partial X_j} \sin k\tau \, \mathrm{d}\tau & \int_0^{2\pi} \frac{\partial Q_i}{\partial X_j} \sin k\tau \cos m\tau \, \mathrm{d}\tau & \int_0^{2\pi} \frac{\partial Q_i}{\partial X_j} \sin k\tau \sin m\tau \, \mathrm{d}\tau \end{bmatrix}$$

$$i = 1, 2, \ldots, N+1, \quad j = 1, 2, \ldots, N+1$$

$$k = 1, 2, \ldots, M+1, \quad m = 1, 2, \ldots, M+1$$

ACKNOWLEDGEMENTS

The financial support from China Southwest Architectural and Research Institute is gratefully acknowledged.

REFERENCES

1. N. Mostaghel and J. Tanbakuchi, 'Response of sliding structures to earthquake support motion', *Earthquake Engng Struct. Dyn.* **11**, 729–748 (1983).
2. J. M. Kelly and K. E. Beucke, 'A friction damped base isolation system with fail-safe characteristics', *Earthquake Engng. Struct. Dyn.* **11**, 33–56 (1983).

3. C. J. Younis and I. G. Tadibakhsh, 'Response of sliding rigid structure to base excitation', *J. Engng. Mech. ASCE* **110**, 417–432 (1984).
4. L. Li, 'Base isolation measure for aseismic building in China', *Proc. 8th World Conf. Earthquake Engng.*, San Francisco VI, 791–798 (1984).
5. S. R. Malushte and M. P. Singh, 'A study of seismic response characteristic of structures with friction damping', *Earthquake Engng. Struct. Dyn.* **18**, 767–783 (1989).
6. R. I. Skinner, W. H. Robinson and G. H. Mcwerry, *An Introduction to Seismic Isolation*, Wiley, New York, 1993.
7. J. M. Kelly, 'Aseismic base isolation: review and bibliography', *Soil Dyn. Earthquake Engng.* **5**, 202–216 (1986).
8. J. M. Kelly and H. C. Tsai, 'Seismic response of light internal equipment in base-isolated structure', *Earthquake Engng. Struct. Dyn.* **13**, 711–732 (1985).
9. L. Su, G. Ahmadi, I. G. Tadjbakhsh, 'A comparative study of performances of various base isolation system part II: sensitivity analysis', *Earthquake Engng. Struct. Dyn.* **19**, 21–34 (1990).
10. Tsung-Wu Lin and Chan-chi Hone, 'Base isolation by free rolling rods under basement', *Earthquake Eng. Struct. Dyn.* **22**, 261–273 (1993).
11. V. Zayas and S. Low, 'A simple pendulum technique for achieving seismic isolation', *Earthquake Spectra* **6**, 317–333 (1990).
12. A. Mokha, M. C. Constantinou, A. M. Reinhorn and V. Zayas, 'Experimental study of friction pendulum isolation system', *J. Struct. Engng ASCE* **117**, 1201–1218 (1991).
13. V. Zayas and T. Al-Hussaini, 'Summary of testing of the friction pendulum seismic isolation system, 1986–1993', *Proc. ATC-17-1 Seismic Isolation, Passive Energy Dissipation and Active Control*, Vol. 1, San Francisco, 1993, pp. 377–388.
14. N. Amin, A. Mokha and H. Fatehi, 'Seismic isolation retrofit of the U.S. Court of Appeals Building', *Proc. ATC-17-1 Seismic Isolation, Passive Energy Dissipation and Active Control*, Vol. 1, San Francisco, 1993, pp. 185–196.
15. Jingwen Xue, *Tribology and the Technique of Lubrication*, Weapon Industry Press, 1992 (in Chinese).
16. Xiangyun Huang, 'Test study on structure base-isolated by ball system with restoring property', *Thesis of the Master's Degree*, Xi'an University of Architecture & Technology, Xi'an, China (1996), (in Chinese).
17. Qiang Zhou, 'Experimental study and numerical analysis on structure base-isolated by ball system with restoring property', *Thesis of the Master's Degree*, Xi'an University of Architecture & Technology, Xi'an, China (1997), (in Chinese).
18. S. L. Lau, Y. K. Cheung, 'Amplitude incremental variational principle for nonlinear vibration of elastic system', *J. Appl. Mech. ASME* **48**, 959–964 (1981).
19. Y. K. Cheung, S. L. Lau, 'Incremental time-space finite strip method for nonlinear structural vibrations', *Earthquake Engng. Struct. Dyn.* **10**, 239–253 (1982).
20. Y. K. Cheung, S. H. Chen, S. L. Lau, 'Application of the incremental harmonic balance method to cubic non-linearity systems', *J. Sound Vib.* **140**, 273–286 (1990).
21. C. Pierre, A. A. Ferri, E. H. Dowell, 'Multi-harmonic analysis of dry friction damped system using an incremental harmonic balance method', *J. Appl. Mech. ASME* **52**, 958–964 (1985).
22. Qianli Tian, S. L. Lau etc., 'Dynamic analysis of structures with frictional joints', *Engng. Mech.* **8**, 1–13 (1991) (in Chinese).
23. M. Hoshiya and E. Saito, 'Structural identification by extended Kalman filter', *J. Engng. Mech. ASCE* **110**, 1757–1770 (1984).

